

EVALUATION OF RISK AND POSSIBLE MITIGATION SCHEMES FOR PREVIOUSLY UNIDENTIFIED HAZARDS

William Linzey, Micah McCutchan, and Michael Traskos
Lectromechanical Design Company

Richard Gilbrech, Ph.D.
NASA Langley Research Center

Robert Cherney
Orbital Sciences Corporation

George Slenski
Wright Patterson Air Force Base

Walter Thomas III
NASA Goddard Space Flight Center

Preface

In April 2004, the NASA Engineering and Safety Center (NESC) was commissioned by NASA's Chief Safety and Mission Assurance (S&MA) Officer to review and render a technical opinion on the probability of a catastrophic failure related to this scenario: The Space Shuttle Program (SSP) recognized a zero-fault-tolerant design related to an inadvertent firing of the primary reaction control system (RCS) jets on the Orbiter during mated operations with the International Space Station (ISS). It was determined that an un-commanded firing of an RCS jet could cause serious damage or loss of both the SSP Orbiter and the ISS. Several scenarios were suggested in which an un-commanded firing of the RCS jet is possible [1]. These scenarios include an arc track event in the 28-volt heater circuits that could result in a wire-to-wire short to the adjacent reaction control jet wire. In this worst-case scenario, enough current and power could be applied to activate the reaction control jet valves and fire a thruster. The following report summarizes the work that was sponsored by the NESC as part of their assessment of the Orbiter inadvertent firing of a RCS thruster while attached to the ISS [2].

Introduction

Background

During the life cycle of an aircraft or spacecraft, new information and performance data change (and even invalidate) engineering assumptions that were made during the initial design and development of a platform. This information can affect many aspects of ownership including the validity of any previous safety analyses. In some cases, a new failure mode may be postulated, found to be a significant threat, and appropriate mitigation techniques developed and deployed to reduce the newly discovered threat to an acceptable level. Where necessary, laboratory evaluation may be needed to acquire data to evaluate new risks, solutions, and advance a technical way forward. The development of mitigation techniques to prevent un-commanded firing of the Space Shuttle's primary RCS jets is an example of such a process.

This report presents the results of arc track testing conducted to determine if such a transfer of power to un-energized wires is possible and/or likely during an arcing event, and to evaluate an array of protection schemes that may significantly reduce the possibility of such a transfer. The results of these experiments may be useful for determining the level of protection necessary to guard against spurious voltage and current being applied to safety critical circuits.

It was not the purpose of these experiments to determine the probability of the initiation of an arc track event — only if an initiation did occur could it cause the undesired event: an inadvertent thruster firing. The primary wire insulation used in the Orbiter is aromatic polyimide, or Kapton®, a construction known to arc track under certain conditions [3]. Previous Boeing testing has shown that arc tracks can initiate in aromatic polyimide insulated 28 volts direct current (VDC) power circuits using more realistic techniques such as chafing with an aluminum blade (simulating the corner of an avionics box or lip of a wire tray), or vibration of an aluminum plate against a wire bundle [4]. Therefore, an arc initiation technique was chosen that provided a reliable and consistent technique of starting the arc and not a realistic simulation of a scenario on the vehicle. Once an arc is initiated, the current, power and propagation characteristics of the arc depend on the power source, wire gauge and insulation type, circuit protection and series resistance rather than type of initiation. The initiation method employed for these tests was applying an oil and graphite mixture to the ends of a powered twisted pair wire.

The flight configuration of the heater circuits, the fuel/oxider (or ox) wire, and the RCS jet solenoid were modeled in the test configuration so that the behavior of these components during an arcing event could be studied. To determine if coil activation would occur with various protection wire schemes, 145 tests were conducted using various fuel/ox wire alternatives (shielded and unshielded) and/or different combinations of polytetrafluoroethylene (PTFE), Mystik® tape and convoluted wraps to prevent unwanted coil activation.

Test results were evaluated along with other pertinent data and information to develop a mitigation strategy for an inadvertent RCS firing. The SSP evaluated civilian aircraft wiring failures to search for aging trends in assessing the wire-short hazard. Appendix 2 applies Weibull statistical methods to the same data with a similar purpose.

Experimental Detail

Test Specimen Configuration and Experimental Setup

Twenty-nine different configurations were tested, with five tests per configuration for a total of 145 tests. All test configurations consisted of heater wires and a set of fuel/ox wires. Heater circuits were made of twisted pairs and fuel/ox wires were either two twisted pairs, one twisted quad, or two shielded twisted pairs, as shown in Figure 1. In all tests, the heater circuits and fuel/ox bundles were bundled together and an arc was initiated in the heater wire bundle. The arc was allowed to propagate down the length of the bundle and damage to the fuel/ox bundle was assessed.

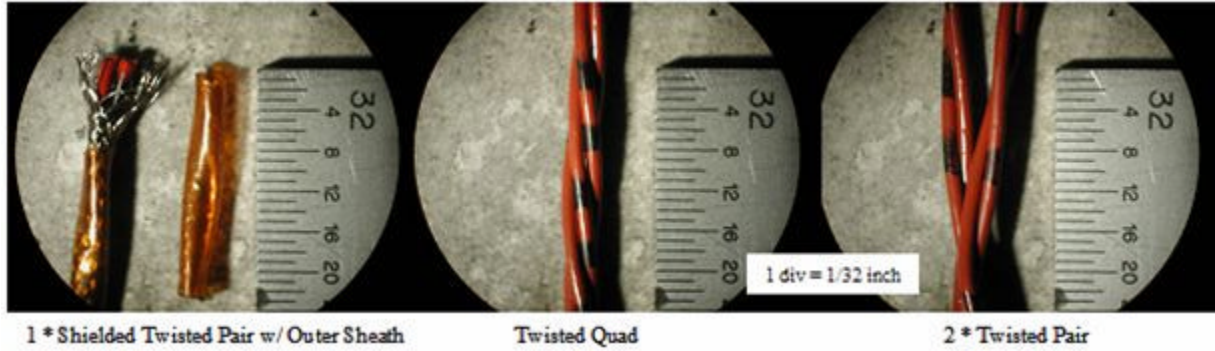


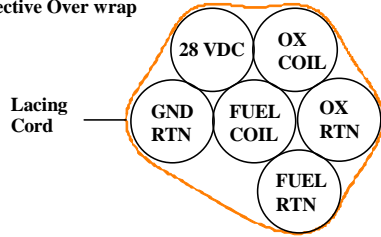
Figure 1. Fuel/Ox Wire Options

Within the set of 145 tests, there were subtle differences in the bundle configurations depending on the number of heater circuits, the type of fuel/ox wire, and the materials used to assemble and protect the bundle. These configurations were grouped into four distinct types, displayed in Figure 2. The application of the protection scheme changed both the size and weight for the fuel/ox bundles. Each protection scheme had a unique impact on the size and weight of the wire bundle. The range of possible configurations is shown in Figure 3.

The type of fuel/ox wire, protection schemes, and circuit protection for each group of five tests are summarized in Table 1. Each protection scheme was applied according to Boeing Orbiter wire harness assembly and installation specifications ML0303-0013D and ML0303-0014N. A description of the twelve different protection schemes evaluated is provided in Appendix 1.

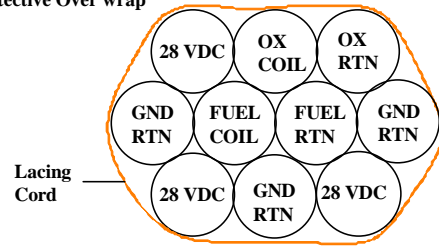
Configuration 1: 1 Power Circuit

Fuel/Ox Wires: Twisted Quad
No Protective Over wrap



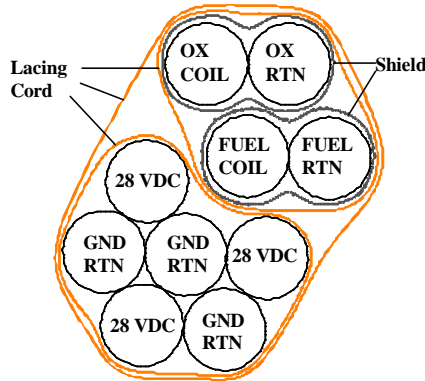
Configuration 1: 3 Power Circuits

Fuel/Ox Wires: Twisted Quad
No Protective Over wrap



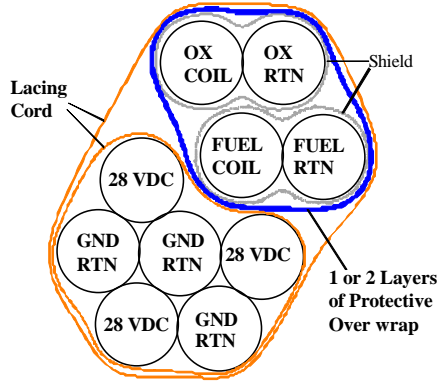
Configuration 2: 3 Power Circuits

Fuel/Ox Wires: 2 Shielded Twisted Pair
No Protective Over Wrap



Configuration 3: 3 Power Circuits

Fuel/Ox Wires: 2 Shielded Twisted Pair
1 or 2 Layers of Protective Over wrap



Configuration 4: 3 Power Circuits

Fuel/Ox Wires: 2 Twisted pair
1 or 2 Layers of Protective Over wrap

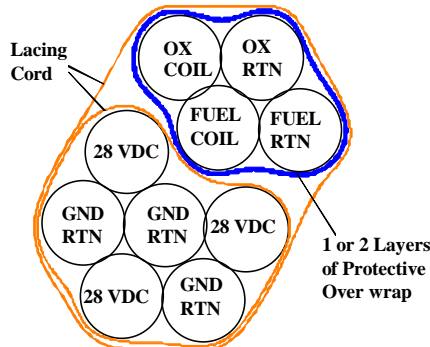


Figure 2. Cross-section of Protection Schemes and Heater Wire Circuits



Shielded Twisted Pair No Protection 1 Layer PTFE Wrap 1 Layer Mystik (3 wraps) 1 Layer Convolute 2 Layers PTFE Wrap 2 Layers Mystik 2 Layers Convolute

Figure 3. Composite Photo of Various Protection Configurations

Table 1. Test Configurations Evaluated

Test #	Harness Config #	# Heater Circuits	Fuel/Ox Wire	Protection Schemes		Circuit Protection (fuse rating)
				1st Layer (Bottom)	2nd Layer (Top)	
N264 1-5	1	1	Twist Quad	NA	NA	15 A
N264 6-10	1	3	Twist Quad	NA	NA	15 A
N264 11-15	2	3	2 Sh/Tw/Pair	NA	NA	15 A
N264 16-20	3	3	2 Sh/Tw/Pair	PTFE Wrap	None	15 A
N264 21-25	3	3	2 Sh/Tw/Pair	Mystik	None	15 A
N264 26-30	3	3	2 Sh/Tw/Pair	Convolute	None	15 A
N264 31-35	3	3	2 Sh/Tw/Pair	PTFE Wrap	PTFE Wrap	15 A
N264 36-40	3	3	2 Sh/Tw/Pair	PTFE Wrap	Mystik	15 A
N264 41-45	3	3	2 Sh/Tw/Pair	PTFE Wrap	Convolute	15 A
N264 46-50	3	3	2 Sh/Tw/Pair	Mystik	PTFE Wrap	15 A
N264 51-55	3	3	2 Sh/Tw/Pair	Mystik	Mystik	15 A
N264 56-60	3	3	2 Sh/Tw/Pair	Mystik	Convolute	15 A
N264 61-65	3	3	2 Sh/Tw/Pair	Convolute	PTFE Wrap	15 A
N264 66-70	3	3	2 Sh/Tw/Pair	Convolute	Mystik	15 A
N264 71-75	3	3	2 Sh/Tw/Pair	Convolute	Convolute	15 A
N264 76-80	4	3	2 Tw/Pair	PTFE Wrap	None	15 A
N264 81-85	4	3	2 Tw/Pair	Mystik	None	15 A
N264 86-90	4	3	2 Tw/Pair	Convolute	None	15 A
N264 91-95	4	3	2 Tw/Pair	PTFE Wrap	PTFE Wrap	15 A
N264 96-100	4	3	2 Tw/Pair	PTFE Wrap	Mystik	15 A
N264 101-105	4	3	2 Tw/Pair	PTFE Wrap	Convolute	15 A
N264 106-110	4	3	2 Tw/Pair	Mystik	PTFE Wrap	15 A
N264 111-115	4	3	2 Tw/Pair	Mystik	Mystik	15 A
N264 116-120	4	3	2 Tw/Pair	Mystik	Convolute	15 A
N264 121-125	4	3	2 Tw/Pair	Convolute	PTFE Wrap	15 A
N264 126-130	4	3	2 Tw/Pair	Convolute	Mystik	15 A
N264 131-135	4	3	2 Tw/Pair	Convolute	Convolute	15 A
N264 136-140	1	1	Twist Quad	NA	NA	10 A
N264 141-145	1	3	Twist Quad	NA	NA	10 A

Each of the four harness configurations, displayed in Figures 4a through 4d, required a slightly different experimental setup. Differential voltage probes and current shunts are included at appropriate locations in the circuits to capture useful information during the arcing event (Figures 4a through 4d). Data were collected on a Nicolet Vision Datalogger at 1 kilosample (KS)/sec.

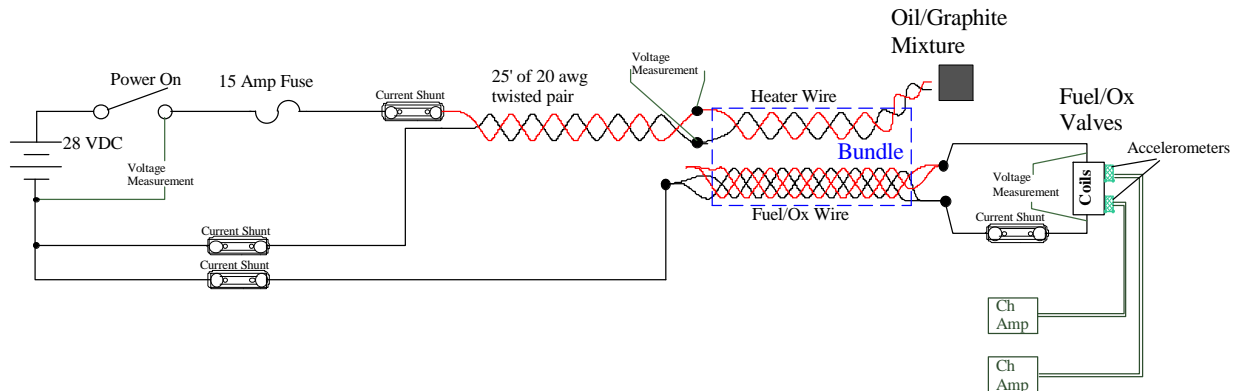


Figure 4a. Harness Configuration 1: 1 Heater Circuit, Fuel/Ox = Unshielded Twisted Quad

Harness configuration 1 (Figure 4a) was the simplest configuration, with only one heater circuit. This configuration was used in Tests 1 through 5 with unprotected twisted quad for the fuel/ox wires. This setup corresponds to the configuration that exists in some locations on the Orbiter.

Fuel/Ox: 1 Twisted Quad

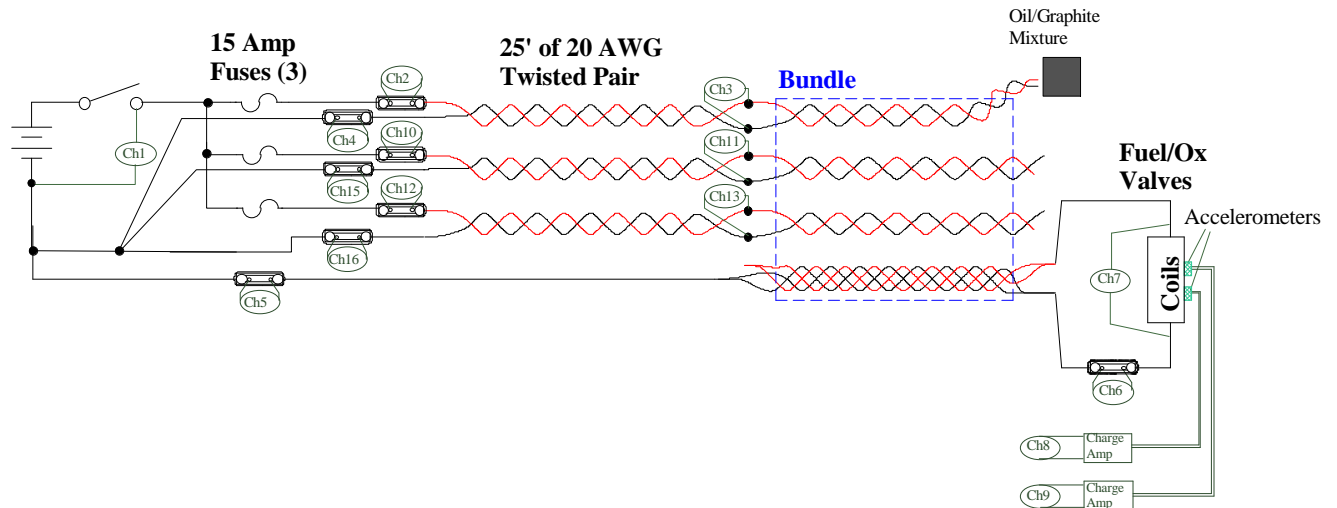


Figure 4b. Harness Configuration 1: 3 Heater Circuits, Fuel/Ox = Unshielded Twisted Quad

Harness configuration 1 with three heater circuits (Figure 4b) was used in Tests 5 through 10 for the unprotected twisted quad. This series of tests represents the configuration that presently exists in some locations on the Orbiter. Tests performed in this group determined whether the present Orbiter configuration would allow enough voltage and current to be transferred to the fuel/ox wires to cause coil activation.

Fuel/Ox: 2 Shielded Twisted Pairs

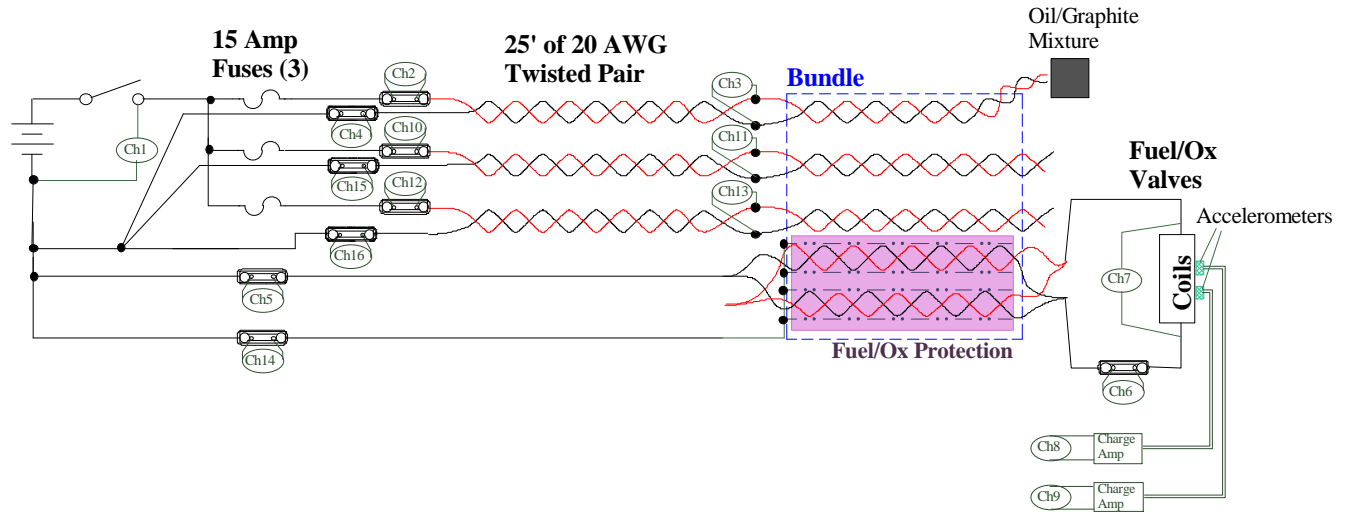


Figure 4c. Harness Configurations 2 and 3: 3 Heater Circuits, Fuel/Ox = Shielded Twisted Pair

Harness configurations 2 and 3, with three heater circuits (Figure 4c), were used in Tests 11 through 75. This series of tests used two twisted shielded pairs for the fuel/ox wires, and included five tests for each of the protection schemes identified in Table 2. Note that the purple box highlights the fuel/ox wires. It should be recognized that each twisted shielded pair had its own metal shield and that one shield does not protect both twisted pairs of fuel/ox wire (see Figures 1 and 2).

Configuration 4
Fuel/Ox: 2 Twisted Pairs

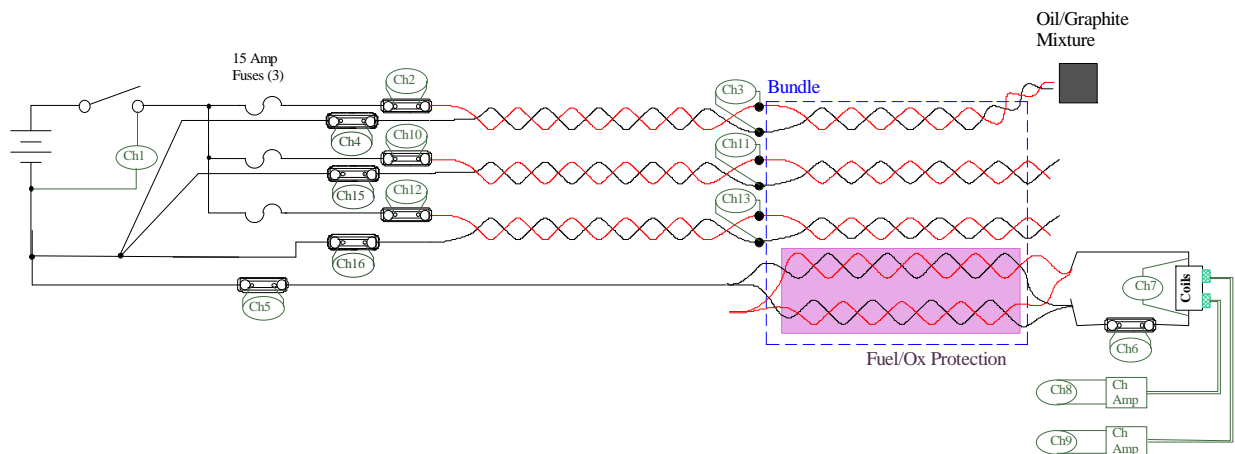


Figure 4d. Harness Configuration 4: 3 Heater Circuits, Fuel/Ox = 2 Unshielded Twisted Pairs

Harness configuration 4 (Figure 4d) was used in Tests 76 through 145. This configuration was essentially the same as configurations 2 and 3, with unshielded twisted pairs replacing the shielded twisted pairs for the fuel/ox wires. This test series included five specimens for each of the protection schemes identified in Table 1.

Heater circuits were represented in the test configurations, but the actual heaters were not. On the Orbiter, the heater switching is located in the fuel/ox valve assembly. Therefore, even when the heaters are off, the heater wires are energized up to the switch at the valve. In this series of tests the heaters were simulated in

the “off” position (open circuit). If the heaters had been included in the test circuit the heaters would have been in parallel with the arc. There would have been little effect on the arc except that the additional heater current would cause the circuit protection to trip earlier limiting the damage.

The 25 feet of 20 American Wire Gage (AWG) (Figures 4a through 4d) wire was used to simulate an event that may occur away from the power bus — this represents the configuration on the Orbiter. The resistance of the 25 feet of wire (~0.25 ohms in both the feeder and return) limits the power in the arc, but also slows the speed that the arc travels and increases the time before the circuit protection (fuse) opens. The later two of these factors tend to increase the collateral damage caused by the arc. While the additional resistance of the 25 feet of wire tends to stabilize the arc, too much resistance (wire) inhibits the arc.

Research into fuel/ox circuits indicated that the aft thrusters are protected, such that “a steady state load current of 15 amperes (amp) shall cause the fusible link to open” (Rockwell Procurement Specification MC477-0263, paragraph 3.4.5). Therefore, the 15 amp fuse was conservative since at this value, the current would not cause the fuse to open. However, without more detailed information, the more conservative protection was used. The forward reaction jet driver (RJD) uses smaller fuses. Therefore, additional tests using harness configuration 1 specimens were performed using 10 amp fuses as protection for the heater circuits.

Test Procedure

After all preliminary checks were performed, the heater circuits were energized and the oil/graphite mixture was used to initiate the arc. The arc was allowed to propagate the length of the sample. The arc event tripped the circuit protection, self-extinguished the arc, or stopped when it reached the end of the sample. After the power was turned off, the specimen was removed from the testing chamber and all test information was recorded. A visual inspection of the sample gave preliminary indications of the effectiveness of the protection scheme. For each sample, wet dielectric voltage withstand (DVW) test was used to determine if the insulation of the fuel/ox wires was actually compromised. Figure 5 is a still shot (captured from video) of Test N264-008 in progress.



Figure 5. Test N264-008 In Progress

The opening of the fuel/ox valve was detected in three ways:

1. Audible clicking sound of valve solenoids.
2. Accelerometer measurements.
3. Coil voltage and current measurements indicating that the coil was at or above the operational threshold.

Damage to the specimen and fuel/ox wire was determined in the following ways:

1. Coil voltage and current measurements (including shield current measurements).
2. Fuel/ox wire damage (visual and wet DVW test).
3. Breach of protection layers (visual examination).

Results

Table 2 summarizes test results with identical harness configuration, protection scheme, and circuit protection grouped together.

Table 2. Test Results Summary Grouped by Experimental Conditions

Test #	Harness Config #	# Heater Circuits	Fuel/Ox Wire	Protection Schemes		Circuit Protection (fuse rating)	Audible Click, Valve Opened	Accelerometer Activity	Max Coil Volt/Current Reading	Damage to Fuel/Ox Wires	Breach of All Protection Layers
				1st Layer (Bottom)	2nd Layer (Top)						
N264 1-5	1	1	Twist Quad	NA	NA	15 A	5/5	Yes	24 V / 2.1 A	Yes	NA
N264 6-10	1	3	Twist Quad	NA	NA	15 A	4/5	Yes	23 V / 2.0 A	Yes	NA
N264 136-140	1	1	Twist Quad	NA	NA	10 A	2/5	Yes	24.8 V / 2.1 A	Yes	NA
N264 141-145	1	3	Twist Quad	NA	NA	10 A	0/5	No	3.5 V / 0.1 A	Yes	NA
N264 11-15	2	3	2 Sh/Tw/Pair	NA	NA	15 A	0/5	No	2.2 V / 0.2 A	Yes	NA
N264 16-20	3	3	2 Sh/Tw/Pair	PTFE Wrap	None	15 A	0/5	No	< 1 V	Slight	4/5
N264 21-25	3	3	2 Sh/Tw/Pair	Mystik	None	15 A	0/5	No	< 1 V	Slight*	2/5*
N264 26-30	3	3	2 Sh/Tw/Pair	Convolute	None	15 A	0/5	No	< 1 V	No	2/5
N264 31-35	3	3	2 Sh/Tw/Pair	PTFE Wrap	PTFE Wrap	15 A	0/5	No	< 1 V	No	0/5
N264 36-40	3	3	2 Sh/Tw/Pair	PTFE Wrap	Mystik	15 A	0/5	No	< 1 V	No	0/5
N264 41-45	3	3	2 Sh/Tw/Pair	PTFE Wrap	Convolute	15 A	0/5	No	< 1 V	No	0/5
N264 46-50	3	3	2 Sh/Tw/Pair	Mystik	PTFE Wrap	15 A	0/5	No	< 1 V	No	1/5
N264 51-55	3	3	2 Sh/Tw/Pair	Mystik	Mystik	15 A	0/5	No	< 1 V	No	0/5
N264 56-60	3	3	2 Sh/Tw/Pair	Mystik	Convolute	15 A	0/5	No	< 1 V	No	0/5
N264 61-65	3	3	2 Sh/Tw/Pair	Convolute	PTFE Wrap	15 A	0/5	No	< 1 V	No	0/5
N264 66-70	3	3	2 Sh/Tw/Pair	Convolute	Mystik	15 A	0/5	No	< 1 V	No	0/5
N264 71-75	3	3	2 Sh/Tw/Pair	Convolute	Convolute	15 A	0/5	No	< 1 V	No	0/5
N264 76-80	4	3	2 Tw/Pair	PTFE Wrap	None	15 A	0/5	No	< 1 V	Yes	4/5
N264 81-85	4	3	2 Tw/Pair	Mystik	None	15 A	0/5	No	< 1 V	Slight	3/5
N264 86-90	4	3	2 Tw/Pair	Convolute	None	15 A	0/5	No	< 1 V	No	1/5
N264 91-95	4	3	2 Tw/Pair	PTFE Wrap	PTFE Wrap	15 A	0/5	No	< 1 V	No	0/5
N264 96-100	4	3	2 Tw/Pair	PTFE Wrap	Mystik	15 A	0/5	No	< 1 V	No	1/5
N264 101-105	4	3	2 Tw/Pair	PTFE Wrap	Convolute	15 A	0/5	No	< 1 V	No	0/5
N264 106-110	4	3	2 Tw/Pair	Mystik	PTFE Wrap	15 A	0/5**	No**	< 1 V**	No	0/5
N264 111-115	4	3	2 Tw/Pair	Mystik	Mystik	15 A	0/5	No	< 1 V	No	0/5
N264 116-120	4	3	2 Tw/Pair	Mystik	Convolute	15 A	0/5	No	< 1 V	No	0/5
N264 121-125	4	3	2 Tw/Pair	Convolute	PTFE Wrap	15 A	0/5	No	< 1 V	No	0/5
N264 126-130	4	3	2 Tw/Pair	Convolute	Mystik	15 A	0/5	No	< 1 V	No	0/5
N264 131-135	4	3	2 Tw/Pair	Convolute	Convolute	15 A	0/5	No	< 1 V	No	0/5

* Specimen N264 – 021 had only 1 wrap of Mystik Tape instead of 3 called for in ML 0303-0014. This shield for this specimen failed the DVW where the shield for the other 4 specimen in this configuration did not.

** Specimen N264 – 106: movement of sample during arc caused Fuel/Ox valve clip lead to touch the heater terminal block and the valve opened. However this was not due to arcing damage or power transferred by the arc. Note: The protection layers were not fully breached.

The background color of the rows signifies the possibility of an arc track event causing the fuel/ox valve to open or caused damage to the fuel/ox wire according to the following:

- **Red:** It is likely that the fuel/ox valve would open due to an arc track event. This would not be an unexpected event should an arc track occur.
- **Yellow:** It is unlikely that the fuel/ox valve would open due to an arc track event; however, significant damage to the fuel/ox wires could be expected.
- **Green:** It is very unlikely that the fuel/ox valve would open due to an arc track event. It is also unlikely that significant damage to the fuel/ox wires could be expected.

The results columns provide the following information:

Audible Click, Valve Opened: When the fuel/ox valve opened and closed, a clicking sound could easily be heard. This column records the number of tests in each group of 5 in which the valve opening/closing was heard.

Accelerometer Activity: The accelerometers, placed on the valve solenoids, were used to “listen” for valve movement. The accelerometer records if movement was detected for any test in the group of 5.

Max Coil Volt/Current Reading: The column shows if there was any electrical activity in the fuel/ox wire even though it was not to an amplitude that opened the valve. If the valve did open at ambient pressure during the test, the current required to open the valve under flight pressure would be higher. These values were used to show that the valve would or would not have opened if it were pressurized. Note: Momentary spikes in voltage and current were not used to determine maximum values.

Damage to Fuel/Ox Wires: Damage indications were the wet DVW test and visual examination. The characterization “Slight” only indicates superficial damage to the insulation.

Breach of All Protection Layers: Determined visually in post-test, this can be used to judge the merit of a given protection scheme.

The considerations that led to the placement of the groups in the red, yellow or green categories follow along with examples of typical test data.

Red: Likely that the fuel/ox valve would open due to an arc track event

The Configuration 1 groups, with unprotected twisted quad fuel/ox wire, were the only ones placed in this category. Eleven (11) of the 20 tests resulted in the fuel/ox valve opening. Table 3 shows data for the individual tests. Both 1 and 3 heater circuit tests caused the valve to open. From this data, it is evident that the 15 amp fuses *allowed* the whole specimen to be damaged without opening while the 10-amp fuse *limited* the arc damage by opening before much damage could occur. In general, the 10-amp fuse would open as soon as the arc entered the main bundle and reached a spot-tie. However, even with the 10 amp fuse limiting damage, it was still possible to have the fuel/ox valve open for durations up to one second due to the arc. While the 3 heater circuit 10 amp fuse group did not cause the fuel/ox valve to open in any of the five tests, it was still placed in this category because of the damage caused to the fuel/ox wire. Also in Test 144, there was arcing directly to one of the coil return wires.

Note: Classical statistical analyses were performed on Tables 3 through 6. It was determined that they do support the trends shown in the tables.

Table 3. Tests Results of the Unprotected Specimens

Test #	Fuse Rating	# of Heater Circuits	Valve Opened? (Audible Clicking)	Len of Arc Dam (inchs).	Fuse Opened			Typical Energized Coil Voltage & Current		Duration Valve Opened (sec)
					H#1	H#2	H#3	V	Amp	
N264 - 001	15 A	1	Y	6	N			24	2.1	4.6
N264 - 002	15 A	1	Y	6	N			18	1.4	1
N264 - 003	15 A	1	Y	7	N			20	0.8	< .05
N264 - 004	15 A	1	Y	6	N			14	1.1	0.8
N264 - 005	15 A	1	Y	8	N			15	1.3	0.9
N264 - 006	15 A	3	Y	8	N	N	N	22	1.9	2.2
N264 - 007	15 A	3	Y	8	N	N	N	10	0.8	0.3
N264 - 008	15 A	3	Y	9	N	N	N	15	1.4	2
N264 - 009	15 A	3	Y	8	N	N	N	21	1.8	0.7
N264 - 010	15 A	3	N	8	N	N	N	5	0.4	NA
N264 - 136	10 A	1	Y	4	N			24	2.0	0.25
N264 - 137	10 A	1	Y	2	Y			24	2.1	1
N264 - 138	10 A	1	N	2	Y			0	0.0	NA
N264 - 139	10 A	1	N	2	Y			15*	0.2*	NA
N264 - 140	10 A	1	N	1	Y			0	0.0	NA
N264 - 141	10 A	3	N	1	Y	N	N	0	0.0	NA
N264 - 142	10 A	3	N	1	Y	N	N	0	0.0	NA
N264 - 143	10 A	3	N	1	Y	N	Y	0	0.0	NA
N264 - 144	10 A	3	N	2	Y	N	N	3.5*	0.1*	NA
N264 - 145	10 A	3	N	1	Y	Y	Y	0	0.0	NA

*The signals oscillated around zero and were most likely from electrical noise generated by the arcing event.

Figure 7 shows the coil voltage and current traces along with the accelerometer reading for Test 008 in which the fuel/ox valve opened. Just before the 26 second mark, ~5 volts (blue line) was measured across the coil with an associated current, < 0.5 amps (red line), measured through the coil. This indicates that the insulation of the fuel/ox wire feeding the high side of the coil was compromised and there was arcing directly to the conductor of that wire. This arcing current returned to ground through the coil with the resistance of the coil (~11.5 ohms) limiting the current. At this voltage/current level the coil was not activated, and the valve remained closed. After ~0.5 seconds the arcing produced a higher voltage across the coil (~12 volts) and the coil activated. The valve opened as recorded by the accelerometers (violet line). Note that the second accelerometer also recorded the opening, but since the traces overlap, it cannot be seen. The voltage across the coil rose to over 15 volts and then collapsed as the fuel/ox return wires also became directly involved in the arc. It was impossible to maintain a voltage across the coil (see discussion of Figure 8 in the next paragraph). The accelerometers also recorded the closing of the valve at about 28 seconds.

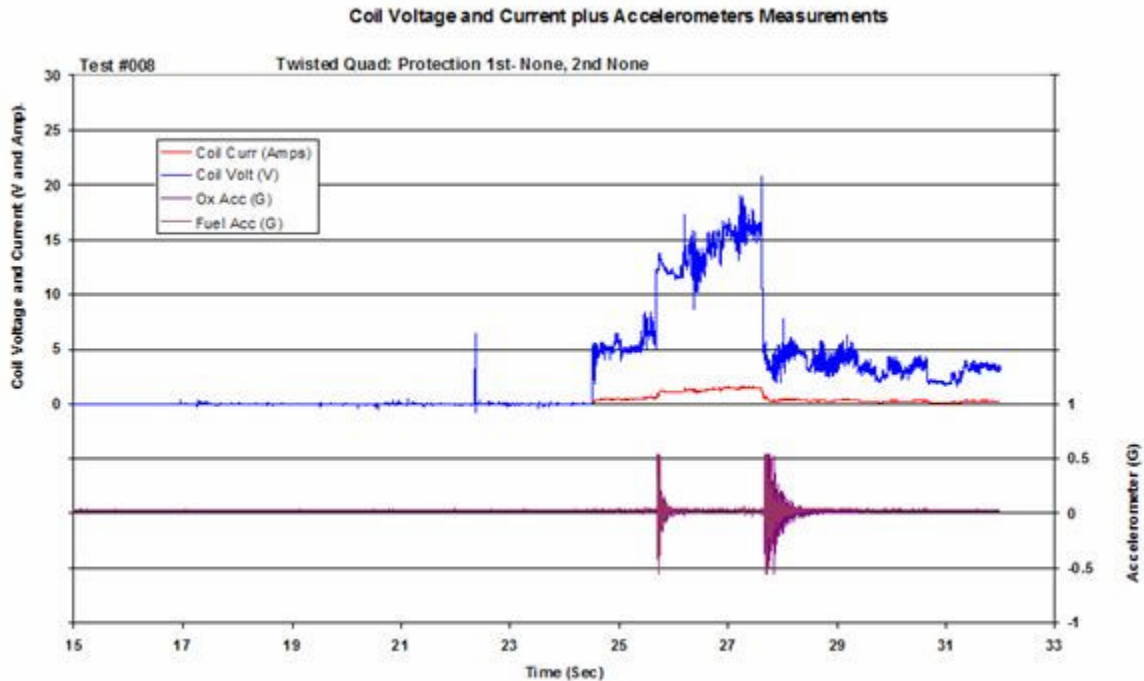


Figure 7. Coil Current and Voltage Traces along with Accelerometer Measurements for Test 008

Figure 8 shows the current (upper traces) and voltage (lower trace) of the arcing wires for Test 8. The darker blue line in the upper trace is the feeder current for the wire in which the arc was initiated (heater #1). The lighter blue line is the return current for heater #1, which by convention is negative. The dark blue line in the lower trace is the voltage at the point when the specimen is attached at the end of the feeder.

Figure 8 also shows the current for the first few seconds of the arc varied greatly, but that it averaged around 15 amps. At this time, the arc voltage (the difference between the dark and light blue lines in the lower traces) was ~ 20 volts. At ~19 seconds, the arc current rose to 40+ amps for 0.6 seconds as the arc propagated through the first spot-tie. Note that the arc voltage was reduced to less than 10 volts as the increased current caused a higher voltage drop in the feeders. This shows the regulatory effect of the feeder resistance because, as the arc current increases, the arc voltage is reduced. The 15 amp fuse did not open at this point because the duration of the current peak was not long enough for this to occur. At the 20-second mark, the return for heater #2 (gold line) became involved in the arc. At this point in time, the heater #1 wire arced to both the heater #1 and heater #2 returns. At about the 22.5 second mark, the heater #3 wire became involved in the arc followed a short time later by the red return. At ~24 seconds, the heater #2 wire also became involved in the event. At this time, the fuel/ox wires had not become involved in the event, but as shown in Figure 7, this changed at ~26 seconds. The activation of the coil can be seen in Figure 8 by observing the slight drip in the fuel/ox return current (green line) as the coil current is returning via the wire. The return current jumps to more than -20 amps, at just over 27 seconds, since there is arcing directly to the fuel/ox return. This causes the coil voltage to collapse and the valve to close.

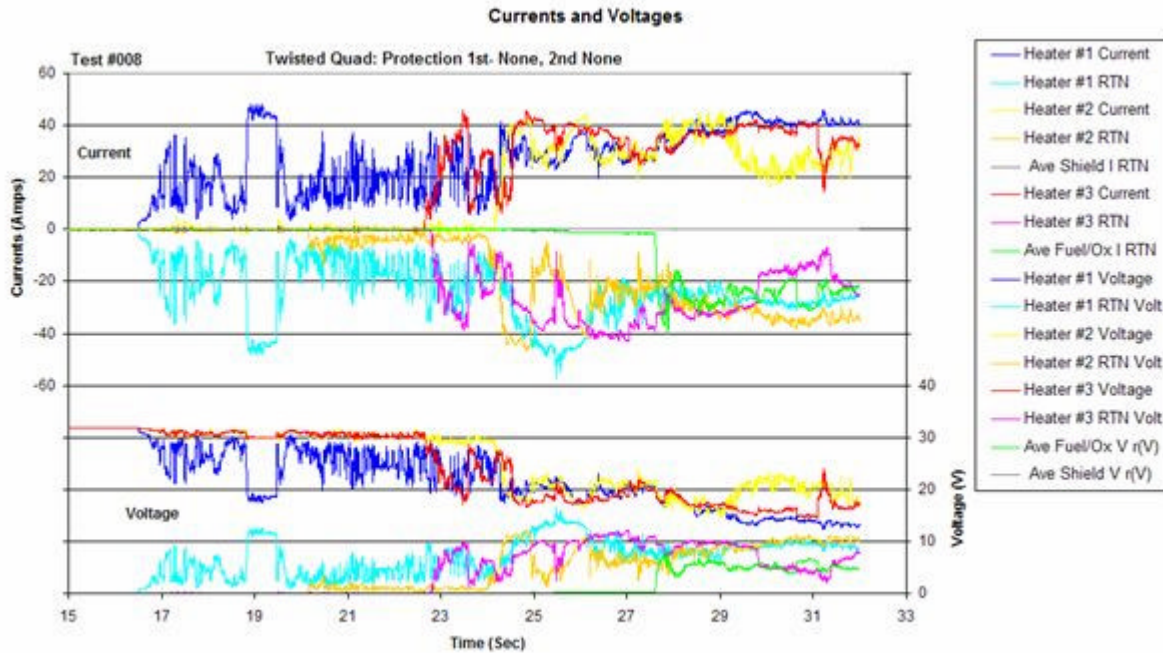


Figure 8. Current and Voltages in the Arcing Event in Test Specimen 008

Figure 9 is the post-test photo of Test Specimen 008 which used 15-amp fuses. The figure shows the extensive damage to both the fuel/ox wire and the heater wire. A section of several of the heater wires have been destroyed (evaporated) in the arc.

Figure 10 shows the post-test photo from Test Specimen 136 which used 10-amp fuses. There is much less damage than in Figure 9, as the 10-amp fuse protected the test specimen. However, there still is significant damage to the fuel/ox wires.

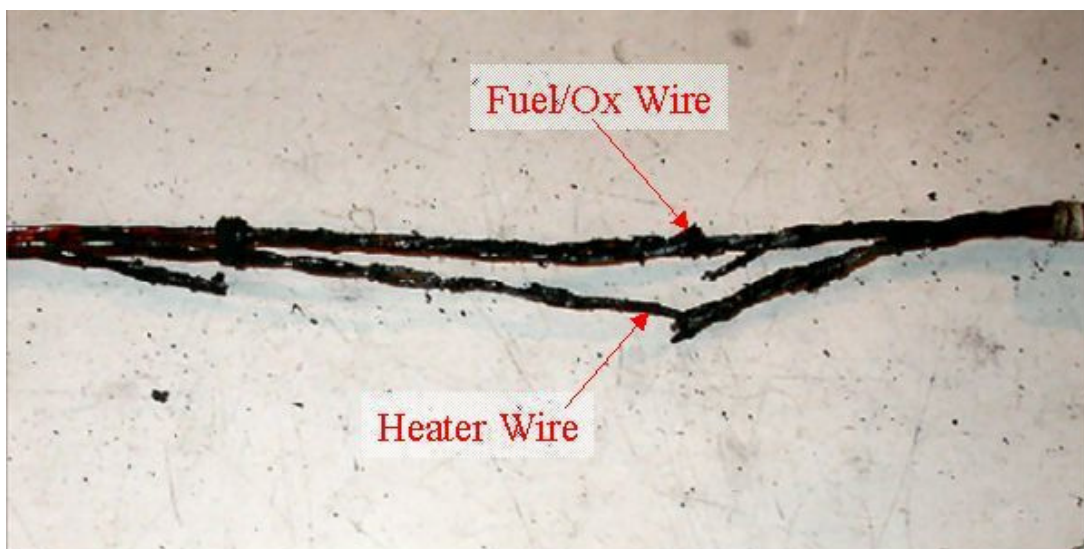


Figure 9. Post-test Photo of Test Specimen 008 (15 amp fuse)

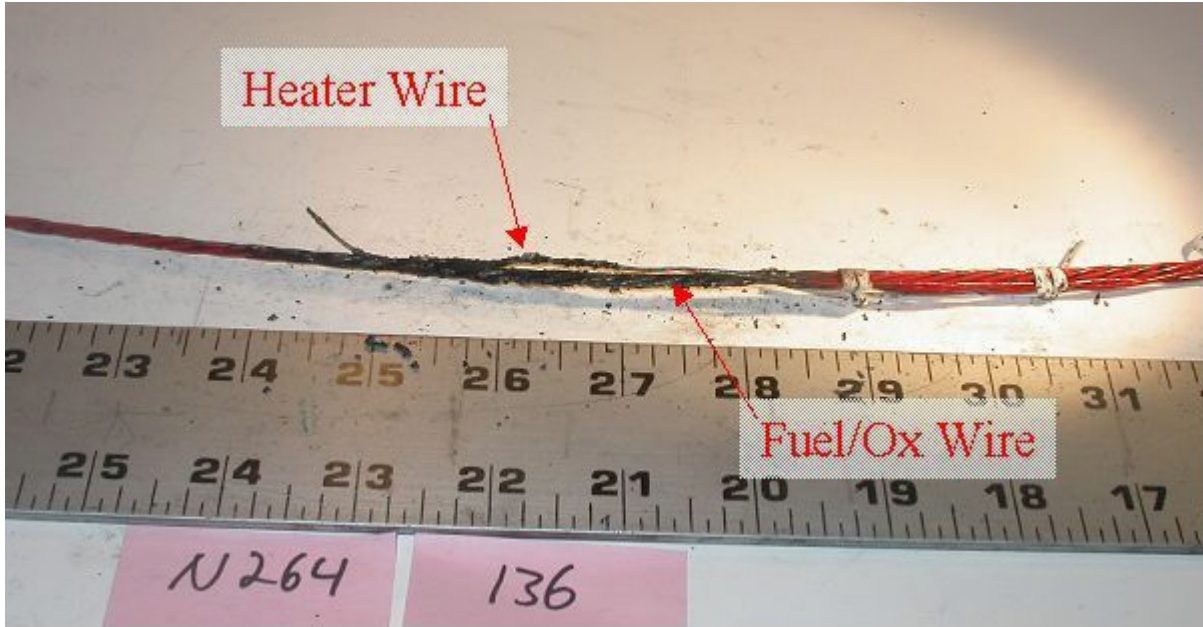


Figure 10. Post-test Photo of Test Specimen 136 (10 amp fuse)

Figure 11 shows a photomicrograph of the damage to the fuel/ox wire of Test Specimen 004. The insulation of the upper wire has been destroyed in the arc and the conductor is exposed. This wire was connected to the high side of the coil. The lower return wires are also damaged and exhibit exposed conductors.



Figure 11. Photomicrograph of Damage to Fuel/Ox Wires

Yellow: Unlikely that the fuel/ox valve would open due to an arc track event

Two groups (011-015 and 76-80) were placed in this category. The fuel/ox wires of the former were unprotected, shielded twisted pairs and the latter were twisted pairs (non-shielded) protected with one wrap of PTFE tape. Figure 12 shows the voltage and current across the coil for Test 012. There is no activity except oscillations of a few volts after the 22-second mark. These oscillations were most likely from electrical noise generated by the arcing event. The fuel/ox wire from Test 012 passed the wet DVW test indicating that there could not have been direct current going from the arc to the fuel/ox wire. Thus, there was only a capacitive/inductive coupled current. The sampling rate of the data logger was too low to obtain frequency information for the oscillations. There is no movement of the valve detected by the accelerometers.

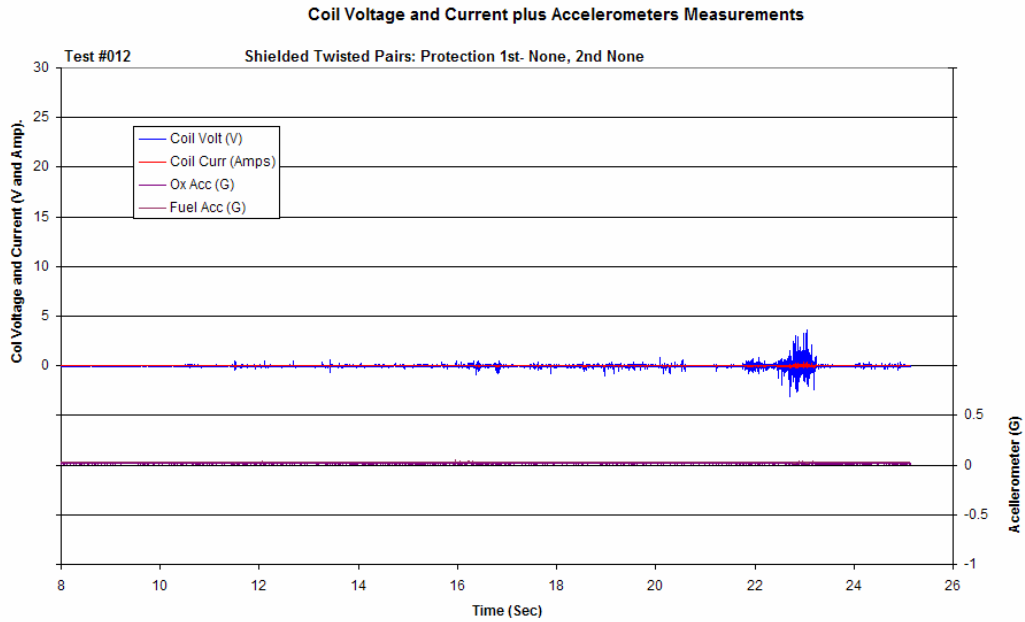


Figure 12. Voltage and Current across the Coil and Accelerometer Measurements for Test Specimen 012

Figure 13 shows the post-test photo of Test Specimen 012. There has been damage to the fuel/ox wires and the shield has been exposed in several places. Because of the heat generated by arcing to the shield, it remains possible that the fuel/ox wire inside the shield may be heat damaged. However, as long as the shield is intact, it is impossible for voltage and current to be transferred from the arc to the inner wires.

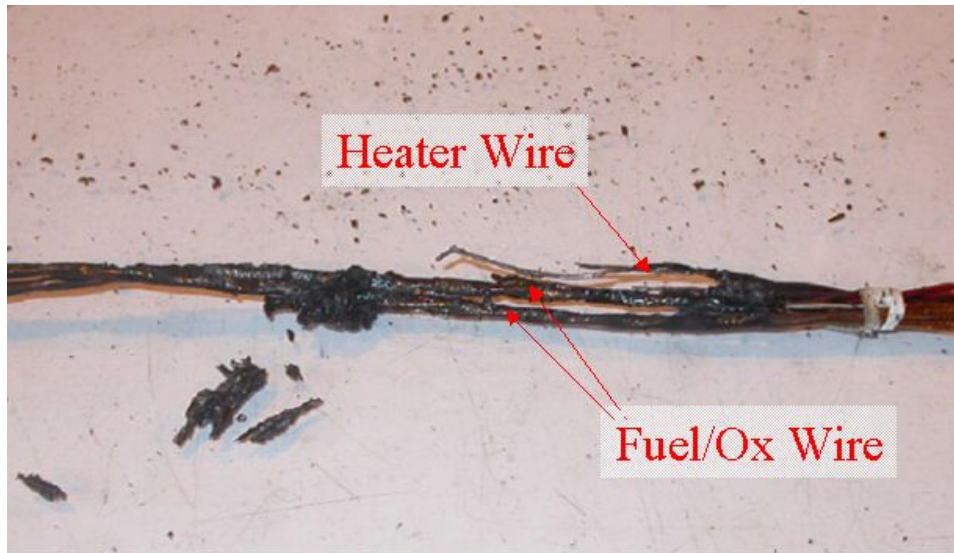


Figure 13. Post-test Photos of Test Specimen 012

Figure 14a shows an example of a breach in the shield. Figure 14b shows damage to an inner fuel/ox wire at the point that it failed the wet DVW test. There is not an obvious breach exposing the conductor, but the insulation had been damage such that it could not prevent current conduction.

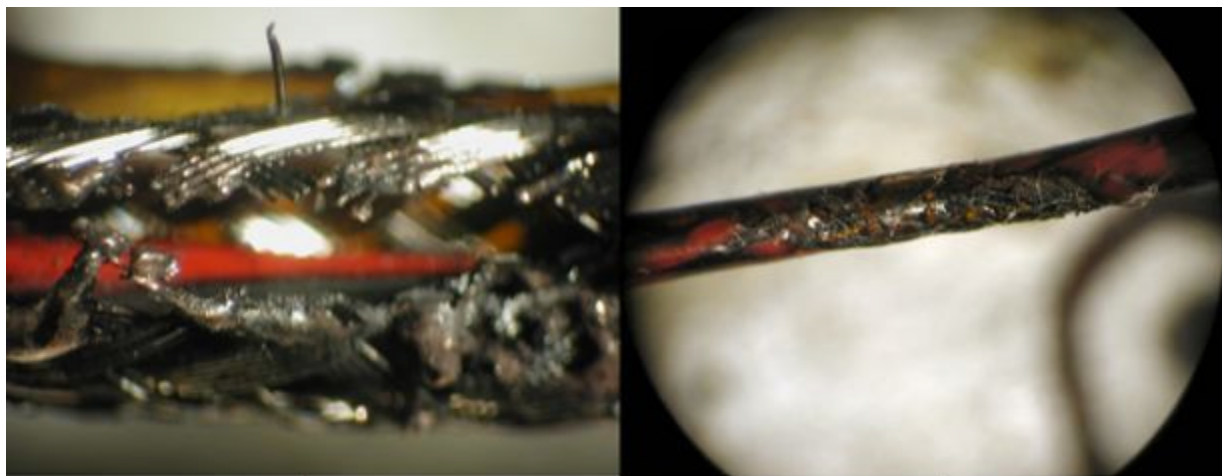


Figure 14a. Close-up of Damaged Shield (Test Specimen 011)

14b. Photomicrograph of the Fuel/Ox Wire at the spot that it failed the wet DWV (Test Specimen 011)

Figure 15 is a photomicrograph of Test Specimen 076. This was the worst-case damage to the fuel/ox wire of any of the protected specimens. Despite the damage, this wire passed the post-test wet DVW as there was still sufficient wire insulation remaining. There was no voltage or current measured across the coil of this specimen and no valve movement detected by the accelerometers.



Figure 15. Post-test Photomicrograph of Fuel/Ox Wire Test Specimen 076

Green: Very unlikely that the fuel/ox valve would open due to an arc track event

The data review for all tests in the green category indicated no voltage or measurable current across the coil. There was no valve movement detected by the accelerometers in any of these tests.

Visual examination of these specimens showed that in many cases the protection did not breach through the protective layers and the fuel/ox wires were in “like new” condition. In some cases, the protection was breached and slight damage occurred to the fuel/ox wire such as spot charring of the topcoat.

Comparison of Effectiveness of Different Protection Materials

A goal of the project was to compare the effectiveness of the different protection materials in preventing arcing damage. For protection of the fuel/ox wires, 120 tests were performed with permutations of PTFE wrap, Mystik® tape wrap, and PTFE convoluted tubing (see Table 2). From these 120 tests, 40 test samples were constructed with each of the protection materials as the top layer of protection. In 10 of the 40 test specimens it was the only layer of protection; in the other 30 test specimens, it was the top layer of a multilayer protection. Test specimens were visually examined after the tests to determine if the top layer of protection was breached completely. Table 4 shows the number of times each material was breached.

Table 4. Top Layer Breaches

Top Layer Material	Number of Breaches	Percent Breached
PTFE	31/40	78%
Mystik® Tape	23/40	58%
PTFE Convolute	12/40	30%

Comparison of Effectiveness of Single and Double Layer Protection Schemes

Table 5, broken-down by single and double layer protection schemes, shows the number of times the protection scheme was breached completely to the fuel/ox wire. As expected, the double layer protection schemes were much more effective in protecting the fuel/ox wire.

Table 5. Comparison Between Single and Double Layer Protection

Description	Single Layer Protection Schemes	Double Layer Protection Schemes
Number of tests in which all layers protection schemes were breached exposing fuel/ox wire	16 of 30 (53.3 %)	2 of 90 (2.2 %)

Comparison of RJD Arc Track Test with Previous Boeing Tests

Table 6 shows a comparison between the RJD tests and those performed previously for Boeing-Huntington Beach [5, 6].

Table 6. Comparison of Results of Previous Tests Performed with those from Current Program

Protection Scheme	Breached All Layers		Wet DVW Failure	
	Previous Tests	RJD Tests	Previous Tests	RJD Tests
None	NA	NA	100% (6/6)	100% (10/10)
PTFE	78% (7/9)	80% (8/10)	44% (4/9)	0% (0/10)
Mystic	67% (2/3)	50% (5/10)	33% (1/3)	10% (1/10) (shield)
Teflon Convolute	100% (12/12)	30% (3/10)	42% (5/12)	0% (0/10)
PTFE/PTFE	50% (1/2)	0% (0/10)	0% (0/2)	0% (0/10)
Mystic/PTFE	0% (0/2)	10% (2/20)	0% (0/2)	0% (0/20)
Teflon Conv/Teflon Conv	14% (1/7)	0% (0/10)	0% (0/7)	0% (0/10)

Several differences observed in the two sets of tests included:

1. The previous tests had 11 or more power wires in the arcing bundle.
2. Typical average arcing currents in the previous Boeing tests were approximately 230 amps compared to 50-60 amps in current RJD tests.
3. In the previous Boeing tests, there was no circuit protection except for 175 amp current limiters on the battery banks.
4. In some cases with the previous Boeing tests, the protection was on the arcing bundle, and not on the target bundle.

5. In the previous Boeing tests, when two applications of protection were used, one application was on the arcing bundle and one application was on the target bundle.

The results show that the higher current levels, and therefore high power in the earlier tests, caused more damage than observed in the present tests. In fact, the higher level of current defeated the single layer protection schemes and in many cases damaged the protected wires. The higher current tests did breach the Teflon® convolute more consistently than the other protection, which is different than the present test results. The double layer protection schemes did provide adequate protection even with the higher current level of the earlier tests, although they could also be breached also. In general, the results of the earlier tests correlate with the present tests when the increase of power of the earlier experiments is considered.

Conclusions

During the life cycle of an aircraft or spacecraft, new failure scenarios are discovered which must be addressed in order to meet safety design requirements. An example is the discovery of a failure condition that could lead to an inadvertent firing of a Space Shuttle RCS thruster when the Shuttle is attached to the ISS. Analysis suggests an inadvertent thruster firing could be catastrophic to both vehicles. In the Orbiter, the thruster valve control wiring is bundled with 28 VDC wiring which has sufficient voltage and current to open a valve and cause the un-commanded thruster firing. This failure scenario only became a safety concern well into the life cycle of the Shuttle. In response to this hazard, a systematic laboratory approach for determining the effectiveness of selected wire protection schemes was developed. The result was a process for electrically isolating Space Shuttle RCS control wiring from adjacent power wiring in the presence of an arc track event. Test results show a single layer of Teflon convoluted tubing or Mystik® tape and, to a lesser extent, PTFE tape is adequate to protect critical wires against moderate current (50 to 60 amps) arcing faults. A double layer protection approach using the three above materials provides the best isolation from adjacent arcing faults and is recommended for high current applications.

References

- [1] Risk Assessment of Wire Failures Causing Uncommanded Orbiter RCS Firing while Docked at the ISS, Datta K., Krause P.A., and Greulich, O.R.
- [2] Space Shuttle Orbiter Reaction Jet Driver (RJD) Independent Technical Assessment/Inspection Report, NASA Engineering and Safety Center (NESC), March 22, 2005. NASA/TM-2005-213750/Version 1. R. Gilbrech et al.
- [3] “Managing Electrical Connection Systems and Wire Integrity on Legacy Aerospace Vehicles,” Paper at the Fourth Joint NASA/ /FAA/DOD Conference on Aging Aircraft, St. Louis, Mo. September 2000. S. Sullivan and G. Slenski.
- [4] Summary Report on the Orbiter Kapton™ Insulated Wire Arc Track Investigation, Report Number N200316JU01, Lectromechanical Design Company for The Boeing Company under contract M0M8XXM-86371M, July 16, 2001, W. Linzey.
- [5] “Convoluted Tube and Teflon Tape Wrap Effectiveness in Redundancy Separation”, Report Number: N202730AP01, Lectromechanical Design Company for The Boeing Company under contract M1M8XXM-863731H, April 30, 2001, W. Linzey.
- [6] “Teflon Convoluted Tube Effectiveness in Redundancy Separation”, Report Number: N204306AU01, Lectromechanical Design Company for The Boeing Company under contract M1M8XXM-863746H, August 1, 2001, W. Linzey.

Appendix 1. Listing of 12 Different Protection Schemes Tested

Fabricated per Space Shuttle Program wiring spec ML0303-0013 and ML0303-0014 (Section 4.1.3 : 'Protection')			
	First (or bottom) Layer	Second (or top) Layer	
1	PTFE Wrap	None	1 Wrap 10 mil PTFE tape: 25-75% Overlap (Section 4.1.3.2.3)
2	Mystik 7503 Tape	None	3 Wraps 4 mil Mystik Tape: 50% Overlap (Section 4.1.3.2.4)
3	Teflon Convolute Tubing	None	1 application 5/8" convolute (Section 4.1.3.2.6)
4	PTFE Wrap	PTFE Wrap	2 Wraps 10 mil PTFE tape (Section 4.1.3.4.3)
5*	PTFE Wrap	Mystik 7503 Tape	1 Wrap 10 mil PTFE (Section 4.1.3.2.3) then 3 Wraps 4 mil Mystik (Section 4.1.3.2.4)
6	PTFE Wrap	Teflon Convolute Tubing	1 Wrap 10 mil PTFE then 1 application 5/8" convolute (Section 4.1.3.4.1)
7	Mystik 7503 Tape	PTFE Wrap	3 Wraps 4 mil Mystik Tape: 50% Overlap then 1 Wrap 10 mil PTFE tape: 25-75% Overlap (Section 4.1.3.4.4)
8	Mystik 7503 Tape	Mystik 7503 Tape	6 Wraps 4 mil Mystik Tape: 50% Overlap (Section 4.1.3.4.5)
9	Mystik 7503 Tape	Teflon Convolute Tubing	3 Wraps 4 mil Mystic Tape: 50% Overlap then 1 application 5/8" convolute (Section 4.1.3.4.2)
10*	Teflon Convolute Tubing	PTFE Wrap	1 application 5/8" convolute (4.1.3.2.6) then 1 Wrap 10 mil PTFE tape (Section 4.1.3.4.3)
11*	Teflon Convolute Tubing	Mystik 7503 Tape	1 application 5/8" convolute (Section 4.1.3.2.6) then 3 Wraps 4 mil Mystic Tape: 50% Overlap (Section 4.1.3.2.4)
12	Teflon Convolute Tubing	Teflon Convolute Tubing	1 application 5/8" convolute then 1 application 1" convolute (Section 4.1.3.4.6)

* These protection schemes are not included in the ML 0303-0013 or ML 0303-0014 specifications.

Appendix 2

Does Civil Aircraft Wiring Exhibit Aging?

Walter Thomas III
 NASA Goddard Space Flight Center
 Greenbelt, Maryland

A previous Space Transportation System (STS) report [1] had reviewed FAA wiring incidents involving civil aircraft to estimate wiring short circuit statistics. Wiring short circuit incidents were counted to derive an occurrence statistic. This provides only a frequency of occurrence – the number of failures per some time interval; no information on how or if failures vary over time (infant mortality, random, or wear-out) results. To accomplish that, one needs to know when events occur (with respect to a relevant time scale) and determine whether failures are decreasing, not changing or increasing with time. The Weibull distribution is ideally suited for determining failure character as the plot slope will show the failure rate as decreasing, increasing, or not changing, given a credible statistical fit.

Weibull analyses on civil aircraft wiring incidents were performed in a previous Shuttle wiring report [2]. Those data were updated for civil aircraft operated in air carrier service with records taken from the FAA Aircraft Incident Database System (AIDS).^{*} Search keywords were: “short,” “shorted,” “shorting,” “short circuit,” “wire,” and “wiring”. Data included incidents from 1978 to 2005. Connectors are a wiring component, so connector events were included. Only air carrier/commercial and air taxi/commuter incidents were used. Each incident was reviewed for *relevance* and *consequence*[†]; duplicate events were removed. Table I summarizes the records reviewed and used by the author for Weibull analyses.

Table I. Summary of FAA AIDS Wiring Damage Occurrences

Keyword	Air carrier/ commercial	Air taxi/ commuter	Total “hits”	# relevant & non-con- sequential	# avail. for Weibull analyses
Short	185	128	313	-	-
Shorted	97	81	178	-	-
Shorting	9	5	14	-	-
Short circuit	5	3	8	-	-
				97	31
Wire	137	176	313	-	-
Wiring	62	25	87	-	-
				153	61
Total	495	418	913	250	92

All wiring failures (broken, chafed, loose, shorted and “other” failures; 250 relevant occurrences, 92 usable for Weibull) are shown in Figure 1. These data fit a Weibull distribution well (Pve =41.6%[‡]). For *all* wiring failures, air carrier aircraft show “early wear-out” failures as indicated by a Weibull slope ($\beta = 1.3$) greater than one.

^{*} <http://www.nasdac.faa.gov/>

[†] *Relevance* means that the incident reflect a wire event; for example, “short” returned aircraft landing short of the runway incidents and “wire” returned “struck a wire on take-off,” etc. A *consequential* event is a wire failure resulting from a cause other than wire deterioration with age; for example shorts caused by fire, liquid contamination, overstress, or another component failing.

[‡] “Pve” is P-value estimate indicating goodness of fit; a Pve greater than 10% indicates a good Weibull fit.

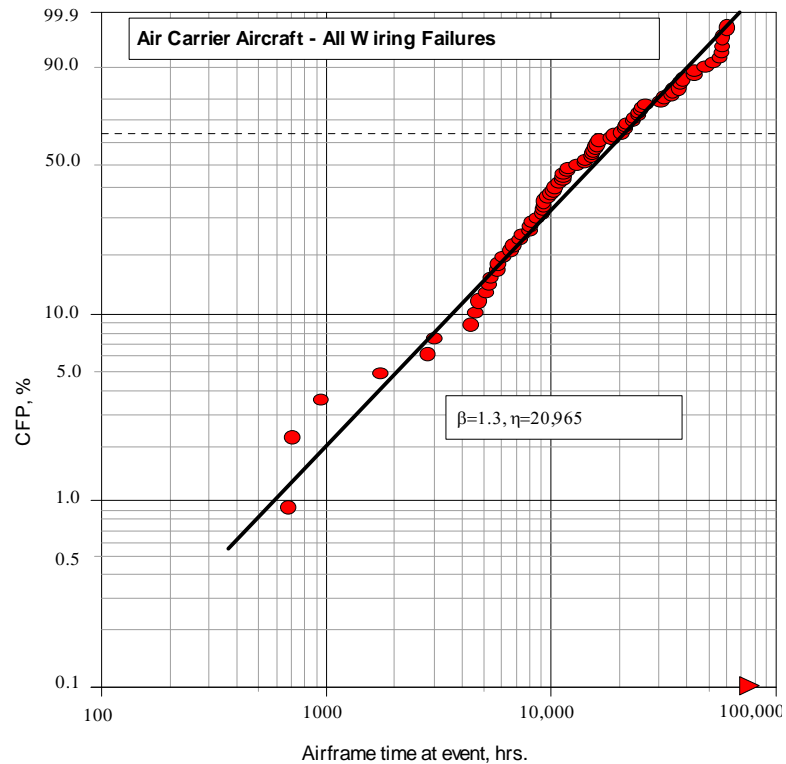


Figure 1. Weibull Plot of ALL Wiring Failures on Air Carrier Aircraft

Weibull analyses typically are performed “one failure mode at a time”. That is, mixtures of failure modes can confound the data. Although Figure 1 does exhibit a good statistical fit, there is some indication modes are mixed: several lower points diverge from the main (center) distribution as do the last upper (longest time) points. Thus data were analyzed further using separate failure modes.

Broken wires (94 failures) initially showed a good two-parameter fit (Pve = 12.5%) with early wear-out failures ($\beta = 1.5$) indicated. However, the first failure (at 1754 hours) strongly influenced the distribution. This broken wire occurred in a B737-700 causing an engine fire. Its early occurrence suggested infant mortality. Censoring this datum yielded a poor two-parameter fit (1.5%), but the curved shape suggested a three-parameter Weibull distribution. A three-parameter fit was excellent (99.9%) with $\beta = 0.90$ and $\eta = 39,800$ hours indicating nearly random failures ($\beta \sim 1$), as shown in Figure 2. Time offset (γ) was 4,433 hours, that is, 4400 hours passed before the broken wire failures commenced.

Wire chafing failures (22, 14 usable for Weibull) showed an increasing failure rate indicative of early wear-out failures: $\beta = 1.25$ and $\eta = 27,400$ hours (Pve 56%). Loose wires occurred as near-random failures ($\beta = 0.93$ and $\eta = 29,100$ hours, Pve 58%).

The initial analysis for shorted wires (97, 31 Weibull usable) indicated early wear-out failures ($\beta = 1.5$, $\eta = 42,000$ hours, Pve = 52%). This plot showed several breaks with three or four subpopulations. These distributions were separated and plotted, as shown in Figure 3. There are three, possibly four, failure distributions with all showing greater β s (3.4 to 4.5) pointing to wear-out or near wear-out failures. A contour plot (Figure 4) compares three failure distributions within shorted wires: β 's are equivalent (contours overlap along the vertical, beta, axis), but they are separated along the eta (time) axis.

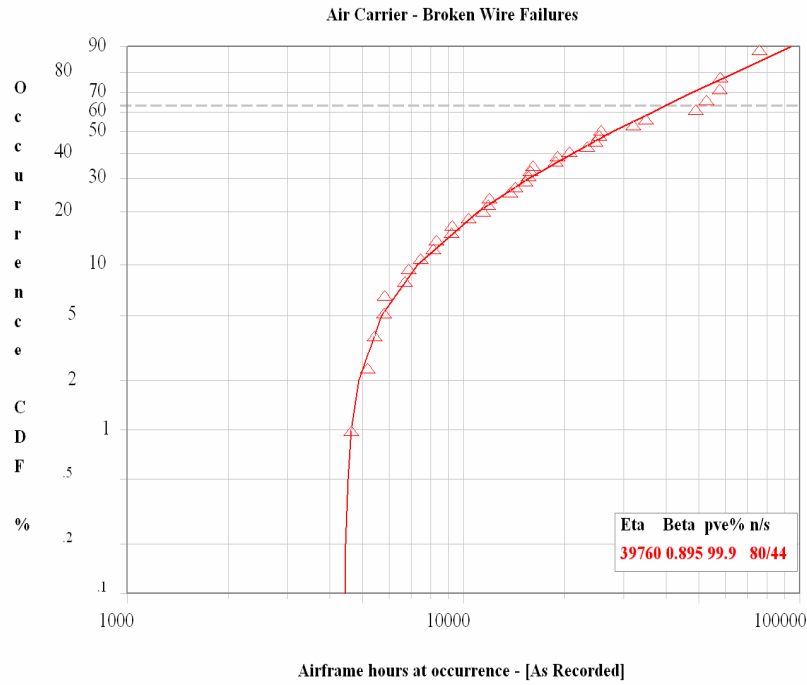


Figure 2. Weibull Plot for Air Carrier Broken Wire Failures

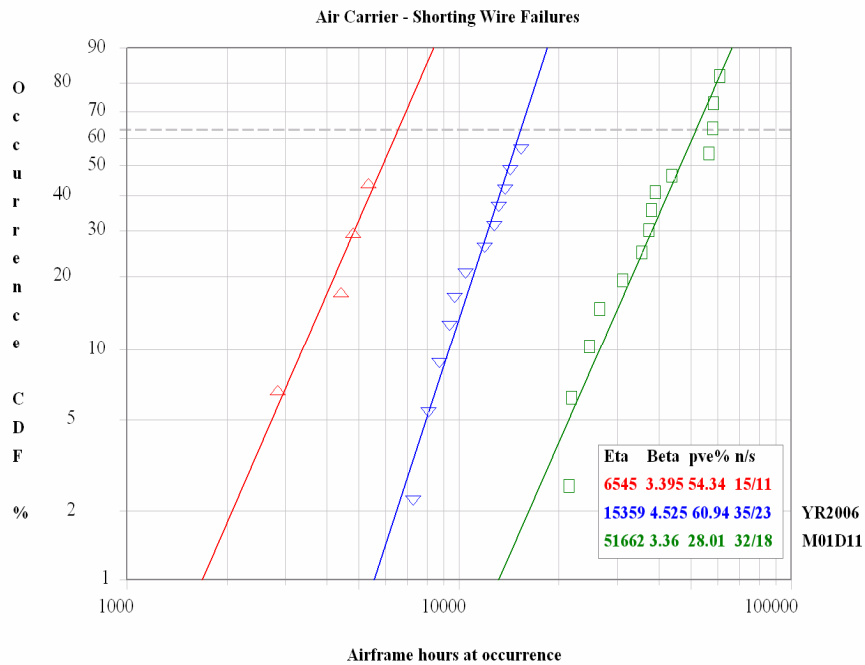


Figure 3. Shorted Wire Failures in Air Carrier Aircraft

As this three distribution model is credible, aircraft wiring shorts likely manifest as wear-out failures distributed over a range of operational times. These several “large β ” distributions combine over a wide time scale to produce an apparent lower- β early wear-out distribution.

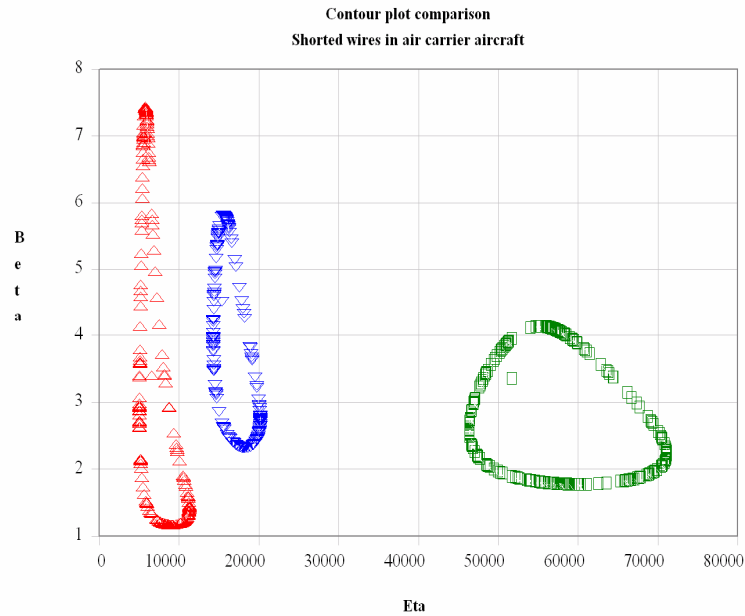


Figure 4. Comparing Weibull Parameters for Shorted Wires in Air Carrier Aircraft (90% confidence intervals)

Helicopters and general aviation type aircraft are used in air carrier/commercial and air taxi/commuter operations. The previous analysis [2] suggested possible differences in wiring failure rates between air carrier (transport) and general aviation aircraft. Additional data in this study was used to test that hypothesis. Weibull data are summarized in Table II.

Table II. Wiring Failure Data for Comparing Aircraft “Classes”

Aircraft Class	n	β	η , hours	Pve, %
Helicopters	8	2.4	7,900	86
General Aviation	25	1.6	8,700	63
Large/Transport	81	1.3	21,000	42

A contour plot (Figure 5) compares these wiring failures. Helicopters and general aviation aircraft wiring failures have β s equivalent to those for large/transport aircraft. However, helicopter and general aviation aircraft failures occurred much sooner – note the distinct separation between *etas* (time axis). Thus general aviation aircraft (and helicopter) wiring failures do occur earlier than those in large aircraft. No cause (why general aviation failures occur earlier) can be determined from these data.

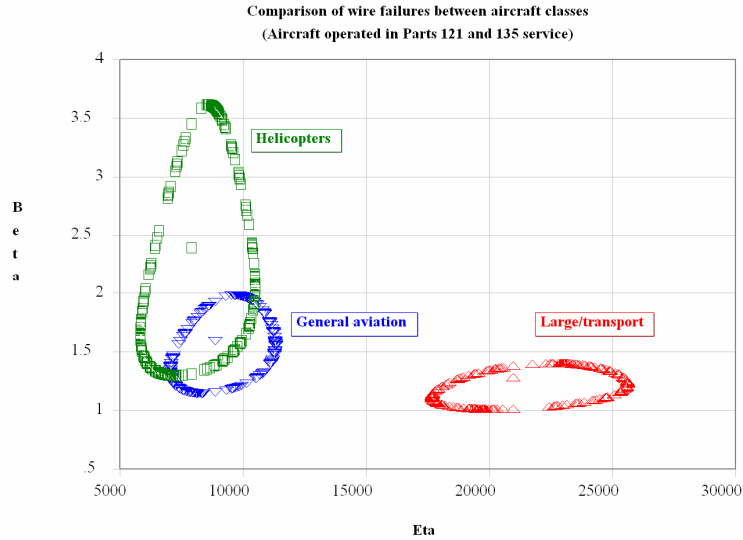


Figure 5. Comparison of Wiring Failure Distributions Between Helicopters, General Aviation and Large/Transport Aircraft used in Air Carrier/Air Taxi/Commuter Service

The above Weibull plots *do not* represent *fleet in-service* failure probabilities. To derive fleet failure probabilities, cumulative “non-failed” (i.e., no wiring failures) operating hours for each aircraft type (those incurring wiring failures) need to be summed. (That data was unavailable in the previous analysis [2]). Adding non-failed operating times (“right censored” data) will drive the Weibull plots down the probability scale and increase characteristic lifetimes (η 's). Slopes should be relatively unaffected [3].

An example illustrates including non-failed operating times. The SAAB SF-340 aircraft was considered. Annual in-flight operating times were taken from the *Transtat* database[§]. Figure 6 is a Weibull plot with and without non-failed operating times (suspensions). Adding non-failed data pushed the failure distribution down the probability axis and slightly diminished its slope. This is expected since adding right suspensions alters the failure ranks. Characteristic life also increased substantially. Another example using data for CE-402 aircraft showed similar results: its bi-modal distribution increased η s (7720 to 15,000 hours and 17,400 to 21,400 hours) and decreased β s (2.2 to 2.1 and 11.5 to 9.3) when non-failed flight hours were added.

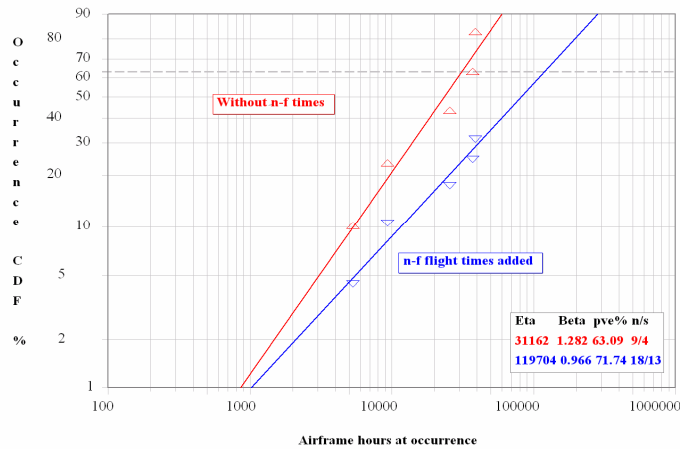


Figure 6. Accounting for Non-Failed Flight Hours, SF-340 Aircraft

[§] <http://transtats.bts.gov/>

Given reliable total annual flight hours for each aircraft type that exhibit wiring failures, complete fleet wiring failure probabilities could be compiled. As that was not the intent of this or the prior work, the example serves to demonstrate what needs to be done to compute true fleet probabilities.

To determine whether wiring is “aging”, one can examine failures over time (i.e., airframe hours at occurrence) and analyze the data using a Weibull distribution. An increasing failure rate — that is, more failures occurring as operating time increases— indicates “aging.” [An analogy is human mortality: people are more likely to die (fail) as they get older (“age”).] Weibull slopes (β s) greater than one show an increasing failure rate; larger slopes (i.e., more than about four) indicate wear-out failures. From one to less than four are “early” wear-out failures. Slopes less than one show infant mortality. For a detailed interpretation, see Reference [3].

In summary, Weibull analyses have shown to be useful for evaluating wiring on aging aircraft. This work, based on FAA aircraft incident records for air carrier, air taxi, commuter and commercial operations over 1978 through 2005 returned over 900 incidents of which 250 were relevant to wire aging. Approximately 90 records contained airframe hours (at occurrence). Subsequent Weibull analyses showed the following:

1. Shorted wires occurred most frequently (153 occurrences) followed by broken wires (120). Chafed and loose wires occurred less frequently, 26 and 13 occurrences, respectively.
2. Air carrier aircraft showed early wear-out wiring failures ($\beta = 1.2$) when **all failures** were combined.
3. Broken wire failures occurred approximately randomly over time ($\beta = 0.9$); characteristic life (η) was 39,800 hours and the “failure-free” time was 4400 hours (three parameter Weibull distribution).
4. Wire chafing occurred as early wear-out failures, with $\beta = 1.25$ and $\eta = 27,400$ hours.
5. Loose wire failures were approximately random ($\beta = 0.93$) with a characteristic life of 29,100 hours.
6. Shorted wires showed wear-out failures having three distributions occurring over 1000 to 60,000 hours with β 's of 3.4 and 4.5. The distributions were distinct and separate.
7. Wire shorts and chafing both showed aging; shorts were wear-out and chafing early wear-out failures.
8. Wiring failures manifested significantly later for large transport aircraft compared to general aviation aircraft and helicopters. General aviation and helicopter wiring failures were similar. Weibull β s were the same for all three aircraft classes.
9. Adding non-failed flight operating times to wiring failures decreases fleet failure probabilities (vs. analyzing failures-only data). Slopes decreased slightly and characteristic lives increased significantly.

Acknowledgements

The author of this Appendix gratefully acknowledges Mr. George Slenski's encouragement to publish these data. Dr. R. Gilbrech, Mr. R. Kichak, Mr. R. Cherney, Mr. G. Williams and Dr. V. Volovoi supported the original study on which this work is based. Dr. R. Abernethy mentored the author and reviewed the original study manuscript. This work was supported by the NASA Engineering and Safety Center through the *Space Shuttle Orbiter Reaction Jet Driver (RJD) Independent Technical Assessment/Inspection*.

References

- [1] S. Roshan-Zamir, Space Shuttle Analysis, SSMA-04-002SAIC, "Space Shuttle Failed-On Thruster Analysis, Probability of Failure Assessment," Safety and Mission Assurance Directorate (NA), Space Shuttle Division (NC), NASA Johnson Space Center, Houston, Texas, Contract Number NAS(-19180, January 9, 2004, 15 pp.
- [2] W. Thomas, III, "Wiring Damage Analysis for STS OV-103," pp. G-1 to G-33 in Appendix G of R. Gilbrech et al, NASA/TM-2005-213750/Version 1, *Space Shuttle Orbiter Reaction Jet Driver (RJD) Independent Technical Assessment/Inspection Report*, NESC Report, March 2005, 155 pp.
- [3] R. B. Abernethy, *The New Weibull Handbook*, Fourth Ed., North Palm Beach, Florida, September 2000, p. 3-5. (ISBN 0-9653062-1-6).